International Journal of Pharmaceutics 389 (2010) 176–185

Contents lists available at ScienceDirect

International Journal of Pharmaceutics

journal homepage: www.elsevier.com/locate/ijpharm

Folate mediated histidine derivative of quaternised chitosan as a gene delivery vector

Viola B. Morris, Chandra P. Sharma*

Division of Biosurface Technology, Biomedical Technology Wing, Sree Chitra Tirunal Institute for Medical Science and Technology, Poojappura, Thiruvananthapuram 695012, Kerala, India

ARTICLE INFO

Article history:
Received 11 November 2009
Received in revised form 20 January 2010
Accepted 23 January 2010
Available online 1 February 2010

Keywords:
Trimethylated chitosan
Histidine
Gene delivery
TEM
Folate receptor targeting

ABSTRACT

Folate targeted gene delivery vectors showed enhanced accumulation in folate receptor expressing tumor model. In the present work, the water solubility and transfection efficiency of chitosans were improved by modifying the depolymerised trimethylated chitosans with histidine moiety. Folate mediated targeting was induced by conjugating poly(ethylene glycol)-folate (PEG-FA) on histidine modified chitosan polymer having low molecular weight of 15 kDa and high degree of quaternisation (HTFP15-H). The zeta potential and size of the HTFP15-H/pDNA nanoparticles were determined using dynamic light scattering technique and the results were confirmed by transmission electron microscopy (TEM). The morphology of the nanoparticles was found spherical in shape having core–shell nanostructure. The HTFP15-H derivative found to buffer in the pH range from 10 to 4. The blood compatibility in terms of percentage hemolysis, erythrocyte aggregation and also by platelet activation was found to be significantly improved compared to the control vector PEI. At a concentration of 10 μg the derivative promote the cell growth up to 139% compared to control at normal cell growing conditions. The transfection efficiency in KB cell line, which over expresses the folate receptor (FR) in presence of 10% fetal bovine serum (FBS) was also found to be comparable to the control. Moreover the enhanced cellular and nuclear uptake due to the conjugation of both folic acid and histidine makes it a potential vector for gene delivery applications.

1. Introduction

Generally two types of vectors such as viral and non-viral, are used for the delivery of nucleic acids in gene therapy. Due to the very high immunogenicity, potential oncogenicity and low DNA loading capacity associated with the viral vectors leads to the development of non-viral vectors as a variable alternative. Significant studies have been done on non-viral gene delivery systems though it may still take some time to reach clinical implementation of human gene therapy (Arote et al., 2007). Safe and clinically efficient gene delivery system can be developed by the use of polymeric matrices that control the rate and location of gene delivery (Megeeda et al., 2004). Because of the high positive charge density and relatively low cytotoxicity, chitosan is considered as an attractive gene delivery vector. Chitosan, the linear cationic polysaccharide, was first described as a delivery system for plasmids by Mumper et al. (1995). The biodegradable cationic polymer chitosan is capable of forming small and stable toroidal complexes with plasmid DNA and provide protection against DNase that is comparable to PEI (Koping-Hoggard et al., 2004). The transfection ability of chitosan was found to be dependent upon many factors such as cell type, serum pH of the transfection medium and the molecular weight of chitosan (Ishii et al., 2001; Corsi et al., 2003). Due to the presence of easily modifiable primary amino group present in chitosan, several research groups have conducted studies using chitosan/DNA nanoparticles, including use of PEI grafted chitosan (Jiang et al., 2007), galactosylated chitosan (Erbacher et al., 1998), galactosylated chitosan-graft-poly(vinylpyrrolidone) (PVP) (Park et al., 2004), trimethylated chitosan oligomers (Thanou et al., 2002), N-dodecylated chitosan (Li et al., 2002), deoxycholic acid modified chitosan (Kim et al., 2001) or ligand attached chitosans for targeting cell membrane receptors (Sato et al., 2001).

Heterocyclic imidazole containing polymers have shown promising transfection efficiency. The imidazole group of histidine plays a pK_a around 6 thus absorb protons and possess buffering capacity in the endosomal pH range (pH 5–6.5). This leads to the osmotic swelling and membrane disruption and eventually the vesicular escape of DNA (Midoux and Monsigny, 1999). The escape of DNA leads to more transfection. This enhanced buffering capacity is due to the lone pair of electrons on the unsaturated nitrogen that provides pH dependent amphoteric properties (Lee et al., 2005, 2008). Many research groups have been studied the improvement in transfection upon conjugation with histidine (Benns et al., 2000;

* Corresponding author. Tel.: +91 4712520214/4712520264; fax: +91 4712341814.
E-mail address: sharmacp@sctimst.ac.in (C.P. Sharma).

0378-5173/$ – see front matter © 2010 Elsevier B.V. All rights reserved.
doi:10.1016/j.ijpharm.2010.01.037

Lee et al., 2007; Bikram et al., 2004; Patchornik et al., 1957; Wang and Huang, 1984). Lee et al. (2003) established the amphoteric property and fusogenic activity of the imidazole group and its interaction in endosomal membrane.

It was reported that many human cancer cell surface such as ovarian, lung, breast brain, colon and kidney over expressed folate receptors. Folate receptor present on tumor has been utilized for targeting of anticancer drugs, genes, and radiopharmaceuticals via folate receptor-mediated endocytosis (Low and Lee, 1995; Ross et al., 1994). Many researchers have used folic acid (FA) as a ligand with cationic liposomes (Kamaly et al., 2009) and other polymers such as chitosan (Zheng et al., 2009; Mansouri et al., 2006), poly(L-lysine) (Kim et al., 2005a,b), and polyethyleneimine (Liang et al., 2008). In one such study, poly(L-histidine) based micelles were conjugated with ligands such as folic acid to enhance the tumor uptake by folate receptor-mediated endocytosis (Lee et al., 2005). In our previous study we investigated that chitosan having medium molecular weight (49–51 kDa) and high degree of deacetylation (DD) gave stable uniform sized nanoparticles whereas low molecular weight chitosans in spite of having good affinity towards DNA, form aggregates easily (Morris et al., 2009).

So in the present study we have attempted the unique properties of trimethylated chitosan and the advantages of imidazole ring on chitosan having four different molecular weight such as low (15 kDa), medium (50 kDa), high (85 kDa) and very high (125 kDa) (Supplementary Table 1). From the physicochemical and preliminary biological characterisation of the above derivatives we have selected low molecular weight chitosan having high degree of trimethylation to induce tumor targetability using folic acid. Interestingly, by introducing PEG-FA to the histidine conjugated trimethylated chitosan having molecular weight 15 kDa and high degree of trimethylation (HTFP15-H) has shown higher transfection, very good cell viability, blood compatibility and cellular uptake compared to native HTMC15-H derivative. (Structure of HTFP15-H has given in Supplementary Fig. 1.)

2. Materials and methods

2.1. Materials

High molecular weight chitosan polymer was obtained from CIFT Kochi, PEI (~25 kD linear), methyl iodide and 1-methyl-2-pyrrolidinone (NMP) and histidine were purchased from Aldrich (USA). 1-Ethyl-3-(3-dimethylaminopropyl) carbodiimide hydrochloride (EDC), dicyclohexylcarbodiimide (DCC), N-hydroxysuccinimide (NHS), methylthiazoletetrazolium (MTT), Minimal Essential Medium (MEM), penicillin/streptomycin (5000 Units/ml, 5000 Ag/ml), trypsin/EDTA were purchased from Sigma (USA). Fetal bovine serum (FBS) was obtained from Gibco (USA). Folate-free RPMI 1640 (FFRPMI), YOYO iodide and Hoechst 33342 were obtained from Invitrogen.

2.2. Depolymerisation of chitosan

The low molecular weight chitosans were prepared by oxidative degradation with $NaNO_2$ at room temperature. The detailed procedures were given elsewhere (Mao et al., 2004). Briefly, 1% (w/w) chitosan was dissolved in 1% acetic acid solution under magnetic stirring. When chitosan was completely dissolved, the appropriate amount of 0.1 M $NaNO_2$, was added drop wise and the reaction was performed at room temperature for 3 h. The reaction mixture was subsequently neutralized with 1N NaOH to pH 8.0 to precipitate chitosan. The precipitated chitosan was recovered by centrifugation, washed several times with deionised water, and finally with methanol and dried in vacuum oven at 60 °C for 5 h. The molecular weights of the depolymerised chitosans were determined by the intrinsic viscosity method as described by Kasaai et al. (2000).

2.3. Preparation of N-N-N trimethylated chitosan (TMC) polymer

Trimethylation of chitosan was performed by a method described by Kean et al. (2005). Depolymerised chitosans were dissolved in NMP with 2.4 g of sodium iodide at 60 °C under stirring. Addition of sufficient NaOH (15% w/v; aq) was made to maintain an alkaline environment throughout the reaction. Methylation was produced through nucleophillic substitution by addition of methyl iodide to the solution. Products were precipitated by addition of diethylether:ethanol (1:1 v/v). Precipitates were centrifuged and supernatants were discarded. Products were dried under nitrogen, redissolved in 0.5 M NaCl and precipitated again with diethylether:ethanol, centrifuged followed by thorough washing of the pellet with diethylether/ethanol. Finally, after drying the pellet, the derivative was dissolved in H_2O and freeze dried. The degree of trimethylation was varied by changing the concentration of the trimethylating reagents without changing the time of reaction. The reaction time was kept constant as 120 min. Chitosans having molecular weight of 15 and 50, 85 and 125 kDa were used for trimethylation. Products were characterised by ^{1}H NMR (300 MHz, Spectrospin and Bruker).

2.4. Preparation of histidine conjugated trimethylated chitosan (HTMC)

Histidine conjugated trimethylated chitosans were prepared by EDC/NHS chemistry. Briefly, the acid group of histidine was activated using EDC/NHS for 1 h at room temperature and it conjugated to the amino group of trimethylated chitosans in acetate buffer of pH 6 for 16 h at room temperature. Products were dialyzed (MWCO 12,000 Da) against deionised water for three days to remove un-reacted substrates and then lyophilized. Chitosans having molecular weight 15, 50, 85 and 120 kDa having two different degree of trimethylation were used for the reaction.

2.5. Preparation of HTMC–PEG–FOL (HTFP) conjugate

The HTMC15-H–PEG–FOL conjugate was synthesized according to the method described elsewhere (Kim et al., 2005a,b). Briefly, folate (15 mg, 0.0375 mmol), DCC (7.5 mg, 0.0375 mmol), and NHS (4.25 mg, 0.0375 mmol) were dissolved in anhydrous DMSO. The activation reaction proceeded under nitrogen for 1 h at room temperature. The insoluble dicyclohexylurea was removed by filtration. A hetero-functional PEG derivative (COOH–PEG–NH_2, 44.5 mg, 0.0125 mmol) dissolved in DMSO was added into the activated folate solution. The PEG–FOL conjugate was dialyzed (MWCO 1000) against deionised water to remove un-reacted substrates and then lyophilized. The terminal carboxylic acid group of the COOH–PEG–FOL conjugate (25 mg, 0.0066 mmol) was also activated with DCC/NHS chemistry in DMSO and conjugated to primary amine groups of HTMC15-H derivative (50 mg). The reaction was carried out at room temperature under nitrogen for 1 h. The reacted conjugate was dialyzed (MWCO 10,000) against deionised water and freeze dried.

2.6. Characterisation of the polymers

^{1}H NMR spectra of the trimethylated chitosan, HTMC and HTFP derivative were measured in D_2O using a 300 MHz spectrometer (Bruker Avance DPX 300). FTIR spectra of the TMC and HTMC samples were measured over 4000–400 cm^{-1} on a Shimadzu spectrophotometer. The solution of the modified chitosan in 0.5% HCl

were prepared in a concentration of 1 mg/1 ml and degree of primary amine content was determined according to the procedure described elsewhere (Azzam et al., 2004).

2.7. Acid base titration

Polymer protonation and positive charge generation over the pH range of 10–4 was determined by acid base titration as previously described (Benns et al., 2002). Briefly 1.5 mg of each polymer was dissolved in 25 ml H_2O to give a final concentration of 60 μg/ml. The solution was titrated to pH 10 with 0.1 M NaOH. The solution was then titrated with 0.1N HCl. The pH profile was obtained for each polymer.

2.8. Amplification and purification of pDNA

The pGL_3 plasmid DNA grown in *E. coli* (JM109) cells was purified using Qiagen QIA filter plasmid Mega kit according to the manufacturer's instruction and resuspended in sterilized Milli-Q water. The purity was confirmed by 1% agarose gel electrophoresis and pDNA concentration was measured by UV absorption at 260 nm.

2.9. Preparation of HTMC/HTFP-pDNA nanoparticles

HTMC samples of different molecular weight and different degree of trimethylation was dissolved in 0.5% HCl in a concentration of 1 mg/ml. The solution was filtered through a 0.22 μm. The plasmid DNA was also prepared in the same concentration of 1 mg/ml. Nanoparticles were prepared in 5 mM PBS having pH 7.4 by mixing pDNA 10 μg/ml with appropriate polymer solution at the various charge ratios. The charge ratios (N/P) of chitosan or its derivative/DNA complexes were expressed as the molar ratios of amine group of chitosan or its derivative to phosphate group of DNA. The system was vortexed for 15 s and incubated for 20 min at room temperature for the complete complex formation. HTFP/pDNA nanoparticles were also prepared in the similar way as described above. It was noted that during complex preparation the volume of pDNA was constant and volume of polymer solution was varied to adjust the theoretical charge ratio. All complexes for the characterisation below were prepared in terms of this method unless otherwise stated.

2.10. Determination of particle size and zeta potential

Particle size and zeta potential of the HTMC-pDNA and HTFP/pDNA nanoparticles were determined using Zetasizer Nano ZS (Malvern Instruments Ltd., UK). The particle size and the zeta potential of the nanoparticles were measured 20 min after preparation. The nanoparticles shall be stable at 15–20 min after complexation.

2.11. Transmission electron microscopy

To examine the morphology of the HTFP-pDNA nanoparticles, 10 μL nanoparticles suspension at N/P = 2 was placed on a copper grid, the excess liquid was removed with a piece of filter paper and then the grid was air dried. Samples were visualized with a Hitachi H 7650 instrument at 100 kV.

2.12. Gel retardation assay

Complex formation was evaluated by agarose gel electrophoresis. The HTFP/pDNA nanoparticles were prepared at N/P ratios of 0.25, 0.5, 1, 1.5, 2 and 4, respectively, by varying the concentration of HTFP. The nanoparticles and the naked plasmid were loaded onto a 0.7% agarose gel in Tris–acetate–EDTA buffer at pH 8.0. The samples were run on the gel at 100 V for 30 min. The gel was stained with ethidium bromide and photographed using a Multi-Image TM Light Cabinet (Alpha Innotech Corporation, San Leandro, CA, USA).

2.13. DNase I protection assay and blood plasma protein interaction

HTFP/pDNA nanoparticles at varying charge ratios such as N/P = 0.5, 1, 2, 4 and 6 was incubated for 10 min at 37 °C with 2 units of DNase I. The DNase I was then inactivated by adding ethtylenediaminetetraacetic acid (EDTA) (0.5 M, pH 8) and incubated for 5 min at room temperature. The pDNA integrity was assessed by agarose gel electrophoresis. The interaction of HTFP/pDNA nanoparticles with plasma protein were determined by mixing 5 μL of plasma protein with 10 μL of nanoparticles containing 1 μL of pDNA at optimum N/P ratio by varying the time of plasma interaction such as 0.5, 1, 1.5 and 2 h, respectively. The stability of pDNA was evaluated by agarose gel electrophoresis.

2.14. Ethidium bromide displacement assay

DNA condensation was measured by ethidium bromide displacement assay described earlier (Petersen et al., 2002). Briefly, 0.5 μg of DNA (1 μg/μL) were complexed with 1 μL (0.1 μg/μL) of ethidium bromide. Polymer solution were then added, to the DNA/EtBr complex to achieve monomer unit:nucleotide ratio of 0.2, 0.4, 0.6, 0.8, 1.0, 1.2, 1.4, 1.6, 1.8, 2.0, 2.2, 2.4, 2.6, 2.8, 3.0, 4.0, and 5.0:1, mixed gently and the fluorescence measured using a fluorescence plate reader at 518 nm excitation and 605 nm emission wavelengths. Results are given as relative fluorescence intensity values.

$$\%\,\text{Relative Fluorescence} = \left\{ \frac{\text{Fluorescence (obs)} - \text{Fluorescence (EtBr)}}{\text{Fluorescence (DNA + EtBr)} - \text{Fluorescence (EtBr)}} \right\} \times 100$$

2.15. Blood compatibility

Blood compatibility of HTFP/pDNA nanoparticles were evaluated in terms of hemolysis by the method described elsewhere (Lee et al., 2004). Blood compatibility was again evaluated by RBC aggregation studies. The saline solution of RBC were incubated with HTFP/pDNA nanoparticles. 10 μL of the sample was mounted on a glass slide and visualized through phase contrast microscope (Leica DM IRB, Germany) at 40 times magnification. Since HTFP/pDNA nanoparticles were found to be more compatible with erythrocytes and plasma, it were again tested for platelet activation and complement activation. The experiment was done as per the standard protocol [ISO 10993-4:2002(E)]. The complement activation of the HTFP/pDNA nanoparticles were determined by turbidimetry method assessing the depletion of complement C3. The polymer solutions in normal saline (100 ml) were incubated for 1 h at 37 °C with 100 ml citrated whole blood. The assay was done as per the protocol provided by the kit manufacturers.

2.16. Cell culture

Human nasopharyngeal epidermoid carcinoma cells (KB cells) were maintained in MEM supplemented with 10% FBS and 1% penicillin–streptomycin under conditions of 5% CO_2 and 95% humidity at 37 °C.

2.17. Evaluation of cytotoxicity

The cytotoxicity of the polymers was measured by MTT assay. KB cell lines were used for the study. Cells were seeded in a 24-well tissue culture plate at 5×10^4 cells/well in 800 μL MEM containing 10% FBS. Cells achieving 70–80% confluence after 24 h were exposed to native polymers and the nanoparticles with pDNA in MEM. After 24 h the derivatives in medium were removed and 200 μL of MTT (0.5 mg/ml in MEM) was added and incubated for 4 h under normal growing conditions. After 4 h MTT were removed and 200 μL of DMSO were added into each wells. The well plates were incubated for 30 min at 37 °C. After 30 min absorbance was measured at 620 nm using a plate reader. Cells without polymers were taken as control.

$$\text{Cell Viability} = \frac{[\text{Abs}]_{\text{sample}}}{[\text{Abs}]_{\text{control}}} \times 100$$

Since the HTFP derivatives found to have cell growth promoting property, it was tested for cell viability by varying the concentration of the HTFP samples such as 5, 10, 15, 30, 45 and 60 μg each per well.

2.18. In vitro transfection studies

KB cells were harvested with 0.05% trypsin/0.53 mM EDTA. Cells were seeded at a density of 10^5 cells/well on a 24-well plate. Minimum essential medium (MEM) was exchanged for folate-free RPMI1640 (FFRPMI) supplemented with 10% FBS and 1% penicillin–streptomycin. Folate-free medium with 10% FBS provides a concentration of folic acid similar to the physiological range. The cells were treated with a polymer/pDNA complex solution in 250 μL of RPMI 10% FBS containing 2.5 μg of plasmid DNA at optimum charge ratio for 4 h at 37 °C. After an exchange of fresh medium, the cells were further incubated for 48 h at 37 °C. Then the growth medium was removed, and the cells were rinsed with DPBS and shaken for 30 min at room temperature in 100 μL of Reporter Lysis Buffer (Promega). Luciferase activity was measured by a luminescence assay, and a protein assay was performed using Micro BCA Protein Assay Reagent Kit (Pierce). According to cell lines, 25 μL of the lysate was dispensed into a luminometer tube and the luciferase activity was integrated over 10 s with a 2 s measurement delay in a Hidex Chameleon, Driver Version Plate reader with the prior addition of 50 μL of Luciferase Assay Reagent (Promega). The final results were reported in terms of RLU/mg cellular protein. PEI having molecular weight of 25 kDa and Superfect are used as positive control. A culture having folate replete media such as RPMI with 1 mM folic acid were used as negative control.

2.19. Cellular uptake studies

Two and half hours after transfection with rhodamine-labelled HTMC15-H and HTFP15-H derivative, cells were washed with PBS to eliminate non-specific bindings. Quenching of extracellular fluorescence was performed with 0.4% trypan blue for 5 min. Cellular uptake of complex were analyzed under confocal laser scanning microscope. The percentage of cellular uptake was estimated using FACS. After the incubation period, the cells were washed with PBS twice and incubated for 2 min with 0.4% trypan blue solution to quench extracellular fluorescence. The cells were again washed with PBS. Then it was treated with trypsin–EDTA for 2 min, and was suspended in PBS. Uptake specificity was assessed by incubating the cells with 1 mM folic acid (Sigma), 1 h prior to adding the nanoparticles. The percentage of cells that had taken up nanoplexes was determined by flow cytometry after excitation with a 488-nm argon laser and detection with a 515–545 nm band pass filter. Suspensions were measured on a BD FACSAria cell sorter (BD Biosciences) and 10,000 cells were evaluated in each experiment. Data acquisition and analysis were performed using BD FACSDiva software (BD Biosciences).

2.20. Plasmid trafficking

Since YOYO iodide is a high affinity DNA labelling dye that exhibits fluorescence enhancement on binding to double-stranded DNA, YOYO was used for the investigation of cellular transport of plasmid during transfection. Plasmid DNA was tagged with YOYO by incubating for 30 min and nanocomplexes of HTFP15-H were prepared at N/P ratio 2. The complexes were incubated with KB cells for 6 h and nuclear staining was done with Hoechst 33342. The cells were then viewed under confocal laser scanning microscope using Argon/2 and He/Ne 543.

3. Results

3.1. Physicochemical and preliminary biological characterisation of HTMC derivatives

The physicochemical characterisation of eight HTMC derivatives were demonstrated in Supplementary Fig. 2. The formations of the HTMC derivatives were confirmed by determining primary amino group contents using a colorimetric assay with 2,4,6-trinitrobenzenesulphonic acid (TNBS) and Fourier transform infrared spectroscopy (FTIR). From the result of TNBS experiment (Supplementary Fig. 2A) it was observed that as the depolymerisation increases the degree of primary amine content also increases. Therefore chito 15 has found to have highest degree of primary amine compared to all other depolymerised derivatives. Quaternisation of four depolymerised chitosan derivatives were carried out by varying the mole ratio of trimethylating agents to obtain two different degrees of quaternised products. For example, the product of chitosan of molecular weight 15 kDa having highest degree of trimethylation is referred to as TMC15-H and lowest degree of trimethylation as TMC15-L, i.e. TMC15-L, TMC50-L, TMC85-L and TMC125-L were obtained by using only half the quantity of the trimethylating reagents which have been used for TMC15-H, TMC50-H, TMC85-H and TMC125-H. The extent of reduction of primary amines upon trimethylation was also estimated using TNBS assay. From the Supplementary Fig. 2A, it was observed that the TMC derivatives having high degree of trimethylation exhibited low degree of primary amines. The results were confirmed by the FTIR spectroscopy (Supplementary Fig. 2B). The reaction between amino groups of TMC and carboxyl groups of histidine leads to the decrease in the –OH stretching vibration and C=O bending vibration peaks of carboxyl groups. All HTMC derivatives showed high intensity peaks of primary amino groups at 3434 cm^{-1}. Which also indicated the hydrogen bonded $NH_{(amide)}$ group. The presence of tertiary amino groups was confirmed as the peaks at 2138 cm^{-1}. The peaks in the spectral region 1700–1500 cm^{-1} indicated the amide groups, asymmetric NH_3^+ bending modes as well as imidazole ring. The peaks at 1563, 1065 and 817 cm^{-1} was also due to the presence of imidazole group. It was very interesting to note that, because of high pK_a value of imidazole group, all the HTMC derivatives showed very good buffering capacity compared to PEI. Out of which, HTMC125-L showed very high buffering capacity.

The mixing of plasmid DNA and HTMC derivatives in PBS at pH = 7.4 results in the formation of complex nanoparticles. The zeta potential and diameters of the complex nanoparticles formed at various charge ratios were measured by dynamic light scattering technique (DLS). Table (Supplementary Table 2) shows the particle sizes and zeta potentials of HTMC/pDNA complexes at various charge ratios. All HTMC derivatives showed a similar pattern. At

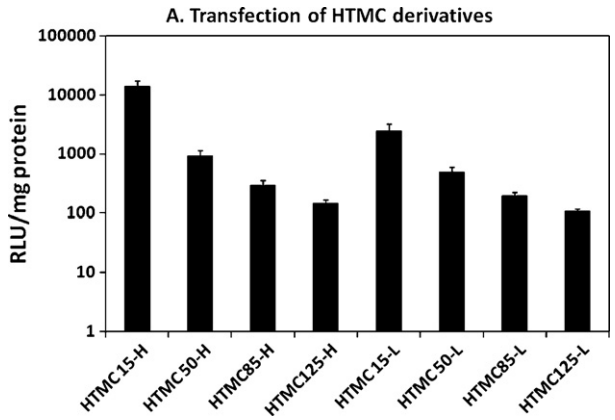

Fig. 1. In vitro transfection of HTMC derivatives into cultured KB oral epidermoid cells. Cells were incubated with polymer/pGL3 complexes (2.5 μg/ml as pDNA) for 4 h in the presence of 10% FBS and then incubated with regular media for 48 h before measurement of luciferase activity. Luminescence activity was measured according to experimental procedures. The luciferase gene expression is represented as relative light units/mg protein (RLU/mg).

N/P = 0.5 particle size was found to be below 200 nm. But at N/P = 1, the size increased to microlevel due to the charge neutrality. Again on increasing the charge ratio, the size was found to be decreasing to below 250 nm and attains a minimum value at N/P = 2.5. The minimum sizes of the derivatives were found to be 230, 212, 291, 179, 231, 205, 213 and 178 nm for HTMC15-H, HTMC15-L, HTMC50-H, HTMC50-L, HTMC85-H, HTMC85-L, HTMC125-H and HTMC125-L, respectively. The zeta potential of HTMC/pDNA complexes in table (Supplementary Table 2) showed that all complexes had a highest zeta potential at charge ratio of N/P = 2.5. Again on increasing the polymer ratio, the zeta potential was found to approaching a plateau and there is not much increase or decrease in the zeta potential. The highest zeta potential of all derivatives were 23.3, 21.6, 24.9, 22.5, 17.2, 17.1, 20.1 and 18.8 mV for HTMC15-H, HTMC15-L, HTMC50-H, HTMC50-L, HTMC85-H, HTMC85-L, HTMC125-H and HTMC125-L, respectively. Due to the minimum size and maximum charge of DNA/polymer nanoparticles was found at the N/P ratio of 2.5, it was taken as optimum for further applications including transfection.

Before doing the necessary biological characterisation of all the HTMC derivatives, transfection efficiency was determined to find out the best derivative at which tumor targeting had to be introduced. From Fig. 1 it was clear that HTMC15-H having low molecular weight and high degree of trimethylation showed highest transfection efficiency compared to all the other HTMC derivatives. So it was selected to induce tumor targetability by conjugating it with PEG-FA.

3.2. Preliminary characterisation of HTFP15-H derivatives and its nanoparticles with pDNA

Modified HTFP derivative was characterised physicochemically using TNBS, IR, ^{1}H NMR, and acid base titration methods. From the figure (Supplementary Fig. 3) it was observed that upon conjugation with PEG-FA, the degree of primary amine content increased. The increase in primary amine was due to the presence of folic acid. This observation was confirmed by IR spectra also. The formation of –NHCO– bonds due to the conjugation of folic acid was confirmed by the presence of high intensity peak at 1639 cm^{-1}. From the Supplementary Fig. 3 it was very interesting to note that, the HTFP15-H derivative buffered in the entire pH range from 10 to 6 while the parent compound HTMC15-H derivative buffered mainly in between 8 and 7. The proton NMR spectra of HTFP15-H derivatives along with its parent polymers HTMC15-H and TMC15-H were given in the Supplementary Fig. 3. The signals at 3.3, 2.9 and 3.5 ppm revealed the presence of protons at trimethylated amino group, dimethylated amino groups and also O-methylated hydroxyl group. From the integral values of signal at 3.3 ppm of trimethylated proton, it is clear that there is a high degree of trimethylation for TMC15-H derivative. The signal at 4.975 ppm at HTMC15-H derivative indicated the presence of proton at imidazole ring of histidine. The presence of PEG group was confirmed from the PEG ($C\mathbf{H}_2C\mathbf{H}_2O$) signals at 3.578 ppm in the NMR spectra. Coupling of the folate residue to PEG grafted chitosan was confirmed by the appearance of signals at 8.1 ppm, which corresponded to the aromatic protons of folic acid. The relevant signals of folate are much weaker than the broad and strong proton signals of PEG and trimethylated chitosan residues.

Table 1
Particle size and zeta potential of HTFP15-H/pDNA nanoparticles. Standard deviation is given in bracket.

N/P ratio	Size (nm)	Zeta (mV)
0.5	284 (14.1)	−27.65 (6.1)
1	1764 (28.2)	−0.88 (0.14)
2	196 (9.8)	15.48 (1.8)
3	284 (8.9)	14.2 (1.1)
4	341 (18.3)	12.58 (0.8)
5	339 (24.0)	12.8 (1.13)

The particle size and zeta potential of HTFP derivative is shown in Table 1. At N/P = 1 the nanoparticles shows very larger size and slight negative charge. Then the size decreased to an average value of 196 nm and corresponding charge was found to be +15.48 at N/P = 2, which was considered as optimum value for further analysis. The size of the complexed nanoparticles was confirmed using TEM micrographs (Fig. 2A). TEM micrographs also revealed the morphology of the nanoparticles. The particles were found to be well known core–shell nanostructure having size less than 100 nm.

The complexes of HTFP/pDNA at charge ratio ranging from 0.25 to 4 were electrophoresed separately in agarose gel. Naked pDNA was used as a control. As shown in Fig. 2B, it was observed that HTFP15-H derivative, effectively retard the plasmid DNA at N/P ratio of 2 and onward. HTFP15-H derivative was examined for DNase 1 degradation and plasma protein interaction using gel electrophoretic shift assay. We performed the degradation experiments at N/P ratios of 0.5, 1, 2, 4 and 6, respectively. Since N/P = 2 was found to be optimum according to DLS method, two ratios above and below were examined to simulate the endosomal environment. Fig. 2C showed that when naked pDNA 1 μg was treated with 2 unit of DNase I (Lane 2), it was completely degraded without any smear (Thakor et al., 2009). The figure further shows that at the same concentration of DNase the pDNA was protected from degradation by the HTFP derivatives much effectively from N/P = 2 an onwards. Below N/P ratio of 2 the protection was not good. Since there was no DNA releasing agents like heparin, the protected pDNA remained in the well and the eroded pDNA moved away from the well. Interaction of plasma proteins on the polymer/pDNA complex was investigated in vitro by incubating the complexed nanoparticles at N/P = 2 with the plasma protein. The extent of pDNA in the complex after interaction with plasma protein was observed using agarose gel electrophoresis. The incubation was done for four periods of time such as 0.5, 1, 1.5 and 2 h, respectively. From Fig. 2C it was clear that even after 2 h the HTFP15-H derivative protect the nanoparticles from disassembly of the complex.

The result ethidium bromide displacement assay is demonstrated in Fig. 3. From Fig. 3 it was observed that the florescence level was above 100% before the addition of HTFP15-H derivatives. On addition of the polymer derivatives it was able to induce the reduction of ethidium bromide fluorescence, which indicates the ability of these copolymers to bind with DNA. From 0 to 1:2.5 both

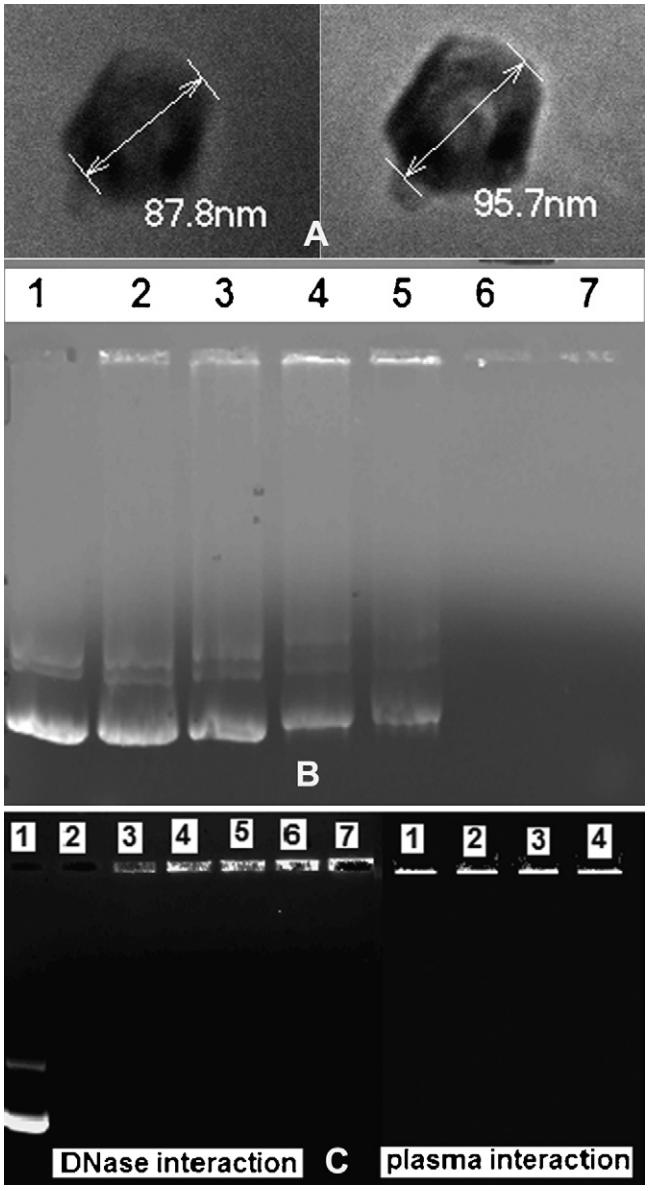

Fig. 2. (A) TEM micrographs of HTFP15-H/pDNA core–shell nanoparticles at charge ratio of N/P = 2. (B) Agarose gel electrophoresis representing pDNA binding studies with eight HTFP15-H derivatives at different N/P ratios. Lane 1: pDNA alone, Lanes 2–7 are HTFP15-H/pDNA at N/P ratios of 0.25, 0.5, 1, 1.5, 2 and 4. (C) Protection of pDNA against DNase I after complexation with HTFP15-H/DNA nanoparticles. Lane 1: pDNA alone; Lane 2: pDNA alone with 2 unit of DNase; Lanes 3–7: HTFP15-H/pDNA at N/P = 0.5, 1, 2, 4 and 6 with 2 units of DNase and interaction of plasma proteins with HTFP15-H/pDNA nanoparticles at N/P = 2. Lanes 1–4: plasma interaction at time intervals of 0.5, 1, 1.5 and 2 h, respectively.

HTMC15-H and HTFP15-H derivative showed an irregularity in the in florescence. After the optimum charge ratio of both the polymer the fluorescence was found to be decreasing steeply and eventually reached a plateau. It may be due to the low binding ability of the polymers until its optimum charge ratio of complexation.

3.3. Blood compatibility and cytotoxicity of HTFP15-H/pDNA nanoparticles

Fig. 4 demonstrates the blood compatibility of HTFP15-H derivatives in terms of erythrocytes lysis and aggregation. For determining the percentage lysis of erythrocytes, 50 μg of the derivatives were used for incubation with erythrocytes for 2 h. DI water and saline solution were used as a positive and negative

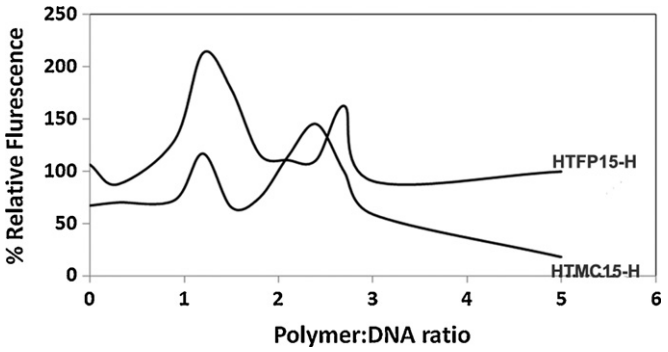

Fig. 3. Ethidium bromide displacement assays for HTMC15-H and HTFP15-H derivatives, at monomer unit:nucleotide molar ratios of 0.2, 0.4, 0.6, 0.8, 1.0, 1.2, 1.4, 1.6, 1.8, 2.0, 2.2, 2.4, 2.6, 2.8, 3.0, 4.0, and 5.0:1.

control, respectively. In the case of HTMC15-H derivatives Fig. 4 demonstrated that hemolysis percentage was higher. However it was observed that upon conjugation with PEG-FA, the hemolysis percentage of HTFP15-H derivative was significantly reduced compared to the parent compound HTMC15-H. Upon complexation with DNA also the hemolysis level was within 15%. So the HTFP15-H derivative was again tested for erythrocyte aggregation and platelet activation. Microscopic images of the erythrocytes were shown in

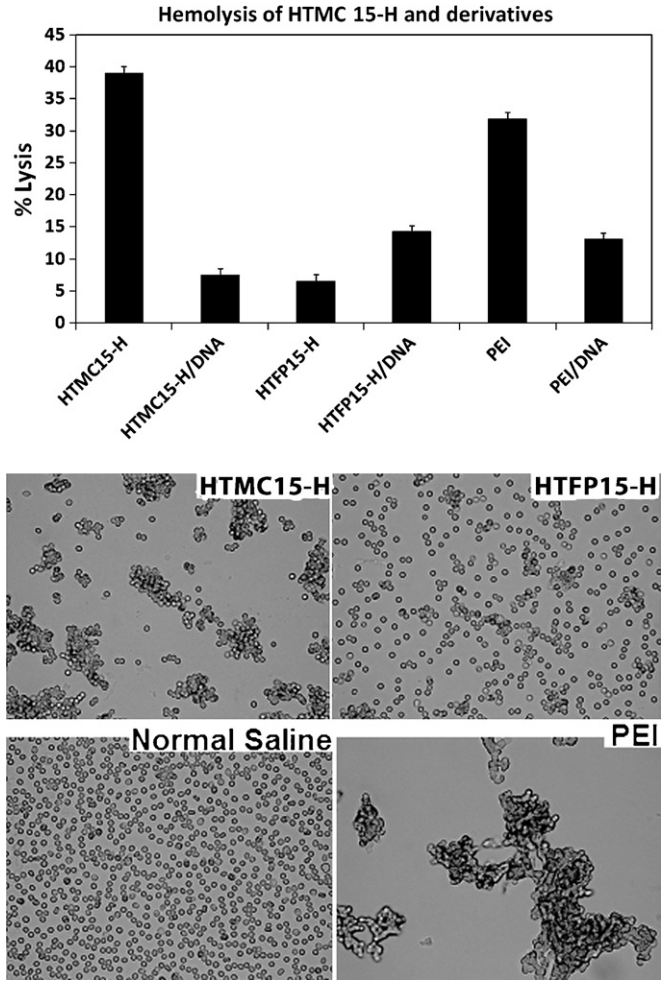

Fig. 4. Hemolysis of HTMC15-H and HTFP15-H derivatives alone and its complex with pDNA; $n = 3$, and RBC aggregation studies with nanoparticles of HTMC15-H and HTFP15-H derivatives with pDNA at a charge ratio of N/P = 3 and 2, respectively (40 times magnification for RBC).

Fig. 4. Nanoparticles were complexed at the optimum charge ratios of respective polymers. From the figure it was very clear to note that upon conjugation with PEG-FA, it behaves more or less similar to that of the reference such as normal saline. That is the HTFP15-H did not cause any RBC aggregation.

It is again reported that cationic polymers induce activation of platelets. To evaluate the platelet activation tendency of the polyplexes they were exposed to platelet rich plasma (PRP) and the percentage of activated platelets were assessed by flow cytometric determination of reduced platelet activation marker P-selectin (CD62). From the results it was observed that there was only 0.025% change in the mean fluorescence intensity of CD62Ab in the HTFP15-H/DNA nanoparticles before and after the incubation of materials compared to PEI with change was about 7.82%, which is a strong activator of platelets. Therefore it was clear that the HTFP15-H polymer did not activate platelets and the values were similar to that of saline control. Complement activation is another major barrier during systemic circulation of nanoparticles. We have used C3 turbidimetry for measuring the complement activation. The consumption of complement C3 is an indication of the extent of C3 activation (Rekha and Sharma, 2009). From the results it is observed that the HTFP15-H nanoparticles with DNA does not activate the complement system. After 1 h incubation with whole blood at 37 °C the HTFP15-H/DNA nanoparticles give 115 mg/100 ml of C3 protein. The value was comparable with the C3 protein content of negative control normal saline such as 128 mg/100 ml.

When the cytotoxicity were measured by complexing the HTMC15-H, HTFP15-H and PEI with DNA in their respective optimum N/P ratios in KB cell lines in which the transfection have been done, it was observed that (Fig. 5A) the cell viability of HTFP15-H/DNA nanoparticles were increased compared to the control. So we have studied the optimum concentration of HTFP15-H derivative which promote maximum cell growth by varying the concentration of the polymer such as 5, 10, 15, 30, 45 and 60 μg each. And it was found that at 10 μg of the HTFP15-H derivatives the KB cell lines showed maximum cell growing property (Fig. 5B)

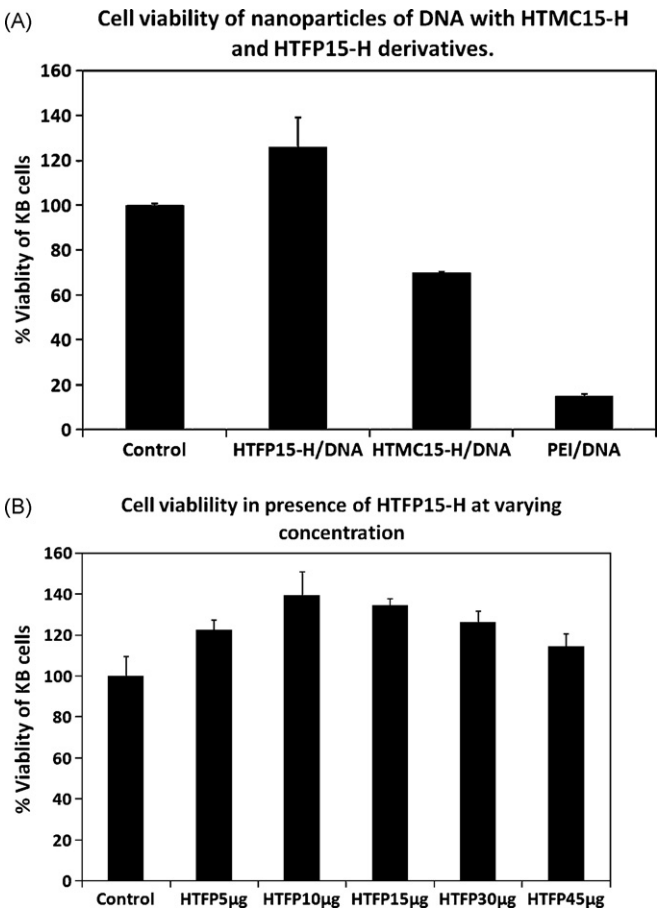

Fig. 5. (A) Viability of KB cell lines at HTFP15-H/pDNA and HTMC15-H/pDNA complexes: $n = 3$, and (B) viability of KB cell lines at varying concentration of HTFP derivatives: $n = 3$.

3.4. Transfection efficiency and cellular uptake of HTFP15-H/pDNA nanoparticles

Fig. 6 shows the transfection efficiency of HTFP15-H derivative in terms of luciferase activity of the protein expressed. It was very interesting to note that even after inducing targetability to the HTMC15-H derivative using PEG-FA, the transfection efficiency was increased significantly compared to its parent polymer. It may be due to the rapid cell internalisation of HTFP15-H derivative in the presence of folic acid to the cells having folate receptor. The specificity of the folic acid conjugated polymeric vector has investigated by doing the transfection experiment in presence and absence of folic acid in the culture medium. For that the culture media is replaced with RPMI having 1 mM folic acid before 1 h of transfection. From Fig. 6A it was observed that due to the competitive displacement of free folic acid the transfection efficiency was decreased to two orders of magnitude compared to the medium without folic acid. We have checked the cell internalisation ability of HTFP15-H derivative compared to HTMC15-H by staining the polymer using rhodamine and observed the internalised nanoparticles after 2.5 h of transfection using confocal microscopy. From Fig. 6B the rapid cell internalisation ability of HTFP15-H was clearly visible compared to HTMC15-H. Since the HTFP15-H polymer had shown rapid cell internalisation compared to the parent compound HTMC15-H, the percentage of cell internalisation was quantitatively estimated using flow cytometry after 4 h of transfection with and without of 1 mmol folic acid inhibitor. The result given in Fig. 7 demonstrated that, 68% of the cell uptake was observed in the absence of folic acid inhibitor. And in the presence of folic acid inhibitor the cellular uptake was reduced to 54%. 10,000 cells were evaluated in each experiment. Since the material was found good for cellular uptake, it is further studied by confocal microscopy for subcellular localisation of polyplexes. Plasmid DNA was labelled using YOYO-1 and incubated with the cells for 6 h. Nuclear staining was done with Hoechst 33342. As found with flow cytometry, the complexes of HTFP15-H derivative were internalised into the nucleus of the cells and uniformly distributed in a high extent (Fig. 7).

4. Discussion

In several approaches, modification of amino groups of polymer using histidine or other imidazole containing structures showed a significant enhancement of gene expression compared to the parent polymer (Midoux and Monsigny, 1999; Fajac et al., 2000; Lo and Wang, 2008). In this work, an effective gene delivery vector has been developed by coupling histidine residues onto the trimethylated chitosan derivatives. Histidine was effectively conjugated to trimethylated depolymerised chitosan (TMC) using NHS/EDC chemistry. TMC derivatives of varying in molecular weight such as 125, 85, 50 and 15 kDa (chito 125, chito 85, chito 50 and chito 15, respectively) were obtained by depolymerisation of the high molecular weight chitosan using sodium nitrite (Mao et al., 2004). The formations of the products were confirmed by using, TNBS method and IR spectra. According to proton sponge mechanism, cationic polymers like PEI are assumed to induce endosomal escape due to the uptake of protons by the amino groups and overall increase in gene transfection efficiency (Lu et al., 2009). One of the

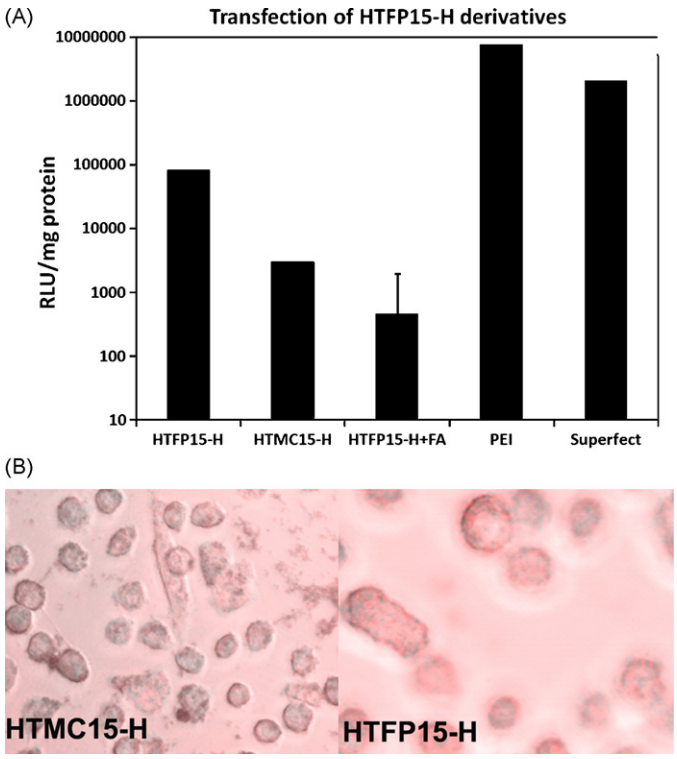

Fig. 6. (A) In vitro transfection of HTFP15-H derivatives into cultured KB oral epidermoid cells. Cells were incubated with polymer/pGL3 complexes (2.5 μg/ml as pDNA) for 4 h in the presence of 10% FBS and then incubated with regular media for 48 h before measurement of luciferase activity. Luminescence activity was measured according to experimental procedures and luciferase gene expression is represented as relative light units/mg protein (RLU/mg). (B) Cellular uptake of polymer/DNA complex. Merged images of light microscope (gray) and fluorescence microscope. Rhodamine-labelled polymer is complexed with DNA and transfected in KB cell lines. The quenching reagent trypan blue was added 2.5 h after transfection.

important factors is that the high density of primary, secondary and tertiary amino groups, which exhibiting protonation only on every third or fourth nitrogen at pH 7 confers significant buffering capacity to the polymers over a wide pH range. By introducing quaternisation and histidine conjugation in chitosan, the presence of primary secondary and tertiary amino groups in the molecule increases which promotes the buffering capacity of the polymer. It was very interesting to observe that all the HTMC derivatives showed much greater buffering capacity compared to PEI.

One of the most important requirements for gene delivery is the formation of complex nanoparticles using the cationic polymers and plasmid DNA. Thus, several parameters affecting the complex formation of the vector with plasmid DNA were examined. Surface charges and size are the two important properties necessary to assure nanoparticles uptake by cells. It was reported that cells typically uptake particles ranging from about 50 to several hundred nanometers (Lu et al., 2009). From the particle size and zeta potential result of HTMC derivatives in Supplementary Table 2 it was observed that at N/P = 1 all the HTMC derivatives showed very large size. At this ratio, for all the derivatives, the zeta potential was found to be almost zero. This effect might probably be due to the "re-entrant condensation" and "charge inversion" (Bordi et al., 2007) occurring in polyion induced aggregation. The ratio at which lowest size and high positive charge were considered as optimum for further studies. For all the HTMC derivatives N/P = 2.5 was found to be optimum.

For inducing tumor targeting property, the derivatives having highest transfection efficiency have been selected out of eight HTMC derivatives. Transfection studies were performed on KB oral epidermoid cells by using pGL_3-Luc as reporter genes in presence of 10% serum. Out of eight HTMC derivatives histidine modified chitosan having low molecular weight and highest trimethylation (HTMC15-H) was found to have highest transfection compared to all the other derivatives (Fig. 1). Since this result was in good agreement with the literature (Koping-Hoggard et al., 2004) we have selected the HTMC15-H for further modification.

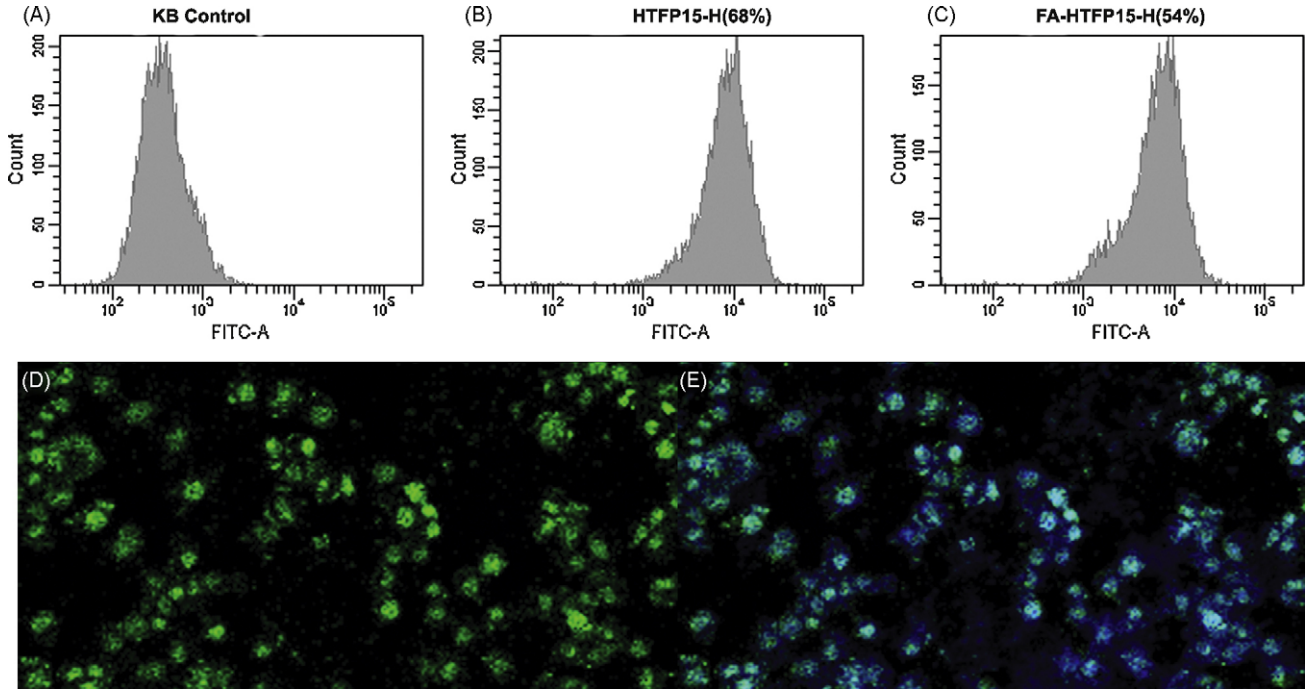

Fig. 7. (A) KB control cell for cellular uptake study of HTFP15-H derivative quantified by flow cytometry in the absence (B) and presence (C) of folic acid inhibitor. (D) Confocal fluorescence microscopic image of YOYO labelled DNA/HTFP15-H nanoparticles in KB cells after 6 h of transfection (green filter). (E) Merged confocal fluorescent microscopic images of Hoechst 33342 stained nucleus (blue filter) and of YOYO labelled DNA (green filter) at the same field. (For interpretation of the references to color in this figure legend, the reader is referred to the web version of the article.)

To introduce tumor targeting efficiency PEG-FA was effectively conjugated to HTMC15-H derivative by DCC/NHS chemistry. The ^{1}H NMR and IR spectra confirm the conjugation of PEG-FA group with the HTMC derivative. From the physicochemical experiment it was observed that in addition to histidine residue due to the presence of PEG folic acid, the buffering capacity of the HTFP15-H derivative has increased significantly. So it may leads to the prolonged endosomal disruption capacity over the entire pH range (Supplementary Fig. 3). The particle size and zeta potential of HTFP derivative was shown in Table 1. At N/P = 1 the nanoparticles showed very larger size and slight negative charge. Then the size decreased to an average value of 196 nm and corresponding charge was found to be +15.48 at N/P = 2, which was considered as optimum value for further analysis. The size of the complexed nanoparticles were confirmed using TEM micrographs (Fig. 2A). TEM micrographs also revealed the morphology of the nanoparticles. The particles were found to be well known core–shell nanostructure having size less than 100 nm.

Physical integrity of the DNA after complexation is a prerequisite for biological activity of the DNA to mediate successful transfection. The ability of HTFP15-H derivatives to form complexes with DNA was confirmed by gel retardation assay. From Fig. 2B it was observed that HTFP15-H derivative, retard the plasmid DNA effectively from N/P ratio of 2 and onwards. This result was in good agreement with the zeta seizer measurement. For a useful gene delivery system, the carriers must be able to protect DNA from degradation by cellular nucleases abundant in serum and extracellular matrix. From Fig. 2C it was clear that from N/P = 2 onwards the HTFP15-H derivative could protect the DNA from degradation by DNase. Fig. 2C also revealed the effect of protection of HTFP15-H derivatives from disassembly of nanoparticles by the influence of negatively charged plasma protein. When an artificial materials were exposed to fluids such as plasma and serum, proteins adsorbed on the surface of the material. It may cause the disassembly of the complexed nanoparticles unless the polymer derivatives are effective for protection. So the aim of our study was to find out any disassembly in the complex in the presence of this negatively charged protein.

Ethidium bromide displacement assay was used to assess the polymer's ability to interact with DNA. It is determined by measuring the change in fluorescence of DNA–ethidium bromide complexes that occurred following the addition of the derivatives. HTMC15-H and HTFP15-H derivatives were experimented using this technique. From Fig. 3 it was clear that after the optimum charge ratio of both the polymer the fluorescence was found to decreasing steeply and reaching a plateau.

In vitro erythrocyte-induced hemolysis is considered to be a simple and reliable measure for estimating blood compatibility of materials (Lee et al., 2004). The behaviour of HTFP15-H/pDNA nanoparticles in vivo can be predicted by examining the degree of hemolysis in vitro. The results (Fig. 4) revealed that due to PEGlation, HTFP15-H derivative become more compatible with erythrocytes than that of the parent compound HTMC15-H. So the derivative was further examined for erythrocyte aggregation platelet activation and complement activation studies. The nanoparticles induced aggregation of erythrocyte under in vitro conditions were analyzed as a prerequisite for the intravenous administration of complexed nanoparticles in animals or humans. The HTFP15-H derivative again showed minimal aggregation potential. The results of platelet activation and complement activation also revealed the negligible activation of platelets and complements. So the enhanced blood compatibility of HTFP15-H derivatives in terms of hemolysis, erythrocyte aggregation platelet activation and complement activation compared to the parent compound HTMC15-H and the positive control PEI might be due to the presence of PEG which protects the cationic sites from interacting with the blood components.

It is reported that cytotoxicity of gene delivery carriers is known to arise from the accumulation of non-degraded and non-discharged polymers with large molecular weight and charge (Lu et al., 2009). MTT assay was used to investigate the cytotoxicity of HTMC15-H and HTFP15-H derivatives in the KB cell lines. The improvement in cell viability of HTFP15-H derivative compared to the control and the parent compound HTMC15-H may again be due to the presence of PEG which reduces the interaction of amine groups with external macromolecules or surfaces (Fig. 5).

To investigate in vitro gene transfer capability of HTFP15-H derivatives, transfection studies were performed on KB oral epidermoid cells by using pGL_3-Luc as reporter genes in presence of 10% serum. FR-expressing KB cells were used as these cell lines are commonly used for folate targeting (Yang et al., 2004; Benns et al., 2002). The gene transfection activity of the polymers was evaluated in terms of luciferase assay, which is a more sensitive method than fluorescence intensity determination (Lu et al., 2009). PEI (25 kDa) has been considered to be the highly effective cationic gene vector, which was used as the control in order to compare the gene transfection efficiency with other non-viral gene vectors. SuperFect, a commercially available gene transfecting reagent, was also used as the control. Culture with excess of free folic acid was used as the negative control over the culture without free folic acid. From Fig. 6A the HTFP15-H derivative showed one and two orders of magnitude more transfection than HTMC15-H and HTFP15-H with excess folic acid, respectively. This decrease in transfection may due to the competitive displacement of the nanoparticles on the folate receptors by excess of free folic acid. In order to confirm the rapid cell internalisation efficiency of targeting group, it was examined using confocal microscopy. Fig. 6B showed rapid cell internalisation of HTFP15-H compared to HTMC15-H. From the flow cytometric analysis given in Fig. 7A revealed the folic acid induced targetability of the HTFP15-H derivative. Again from Fig. 7B, the derivative showed the high level of localisation of plasmid DNA inside Hoechst 33342 stained nucleus after 6th hour of transfection. Since the folic acid conjugated histidine derivative has very good endosomal disruption capacity, it may go through rapid endosomal escape and nuclear uptake.

5. Conclusions

In conclusion, high molecular weight chitosan was depolymerised, trimethylated and conjugated with histidine to introduce enhanced buffering capacity and rapid endosomal disruption, resulting increased transfection efficiency. The HTMC derivatives which exhibited very good transfection efficiency were again modified with PEG-FA to induce tumor targetability. The resulting polymer HTFP15-H when complexed with plasmid DNA, were found to protect DNA from DNase degradation and also from disassembly in presence of negatively charged plasma proteins. It showed improved blood compatibility in terms of percentage hemolysis, erythrocyte aggregation and also by platelet activation. At a concentration of 10 μg the derivative showed very high cell growing property compared to the control at normal cell growing conditions. The transfection efficiency was also found to be comparable to PEI when transfected in KB cell line, which over expresses the folate receptor (FR) in presence of 10% FBS. Due to the conjugation of folic acid and histidine the derivative was found to have enhanced cellular and nuclear uptake compared to the parent polymer.

Acknowledgements

This work was supported by CSIR, New Delhi and FADDS under DST, New Delhi. We express our thanks to Dr. T.V. Anilkumar,

SCTIMST for confocal microscopy, Dr. Lissy K Krishnan, SCTIMST for FACS facility and Dr. Annie John, SCTIMST for TEM studies. Thanks are due to Director and Head for providing facility.

Appendix A. Supplementary data

Supplementary data associated with this article can be found, in the online version, at doi:10.1016/j.ijpharm.2010.01.037.

References

Azzam, T., Eliyahu, H., Makovitzki, A., Linial, M., Domb, A.J., 2004. Hydrophobised dextran-spermine conjugate as potential vector for in vitro gene transfection. J. Control. Release 96, 309–323.

Arote, R., Kim, T.-H., Kim, Y.-K., Hwang, S.-K., Jiang, H.-L., Song, H.-H., Nah, J.-W., Cho, M.-H., Cho, C.-S., 2007. A biodegradable poly(ester amine) based on polycaprolactone and polyethylenimine as a gene carrier. Biomaterials 28, 735–744.

Benns, J.M., Choi, J.S., Mahato, R.I., Park, J.S., Kim, S.W., 2000. pH-sensitive cationic polymer gene delivery vehicle: *N*-Ac-poly(L-histidine)-graft-poly(L-lysine) comb shaped polymer. Bioconjugate Chem. 11, 637–645.

Benns, J.M., Mahato, R.I., Kim, S.W., 2002. Optimization of factors influencing the transfection efficiency of folate–PEG–folate-graft-polyethylenimine. J. Control. Release 79, 255–269.

Bikram, M., Ahn, C.H., Chae, S.Y., Lee, M., Yockman, J.W., Kim, S.W., 2004. Biodegradable poly(ethylene glycol)-co-poly(L-lysine)-g-histidine multiblock copolymers for nonviral gene delivery. Macromolecules 37, 1903–1916.

Bordi, F., Cametti, C., Sennato, S., Viscomi, D., 2007. Radiofrequency dielectric loss relaxation in polyion-induced liposome aggregates. J. Colloid Interface Sci. 309, 366–372.

Corsi, K., Chellat, F., Yahia, L., Fernandes, J.C., 2003. Mesenchymal stem cells, MG63 and HEK293 transfection using chitosan-DNA nanoparticles. Biomaterials 26, 1264–1275.

Erbacher, P., Zou, S., Bettinger, T., Steffan, A.M., Remy, J.S., 1998. Chitosan-based vector/DNA complexes for gene delivery: biophysical characteristics and transfection ability. Pharm. Res. 15, 1332–1339.

Fajac, J.C., Allo, E., Souil, M., Merten, C., Pichon, C., Figarella, M., Monsigny, P., Briand, P., Midoux, 2000. Histidylated polylysine as a synthetic vector for gene transfer into immortalized cystic fibrosis airway surface and airway gland serous cells. J. Gene Med. 2, 368–378.

Ishii, T., Okahata, Y., Sato, T., 2001. Mechanism of cell transfection with plasmid/chitosan complexes. Biochim. Biophys. Acta 1514, 51–64.

Jiang, H.-L., Kim, Y.-K., Arote, R., Nah, J.-W., Cho, M.-H., Choi, Y.-J., Akaike, T., Cho, C.-S., Choi, Y.-J., Akaike, T., Cho, C.-S., 2007. Chitosan-graft-polyethylenimine as a gene carrier. J. Control. Release 117, 273–280.

Kamaly, N., Kalber, T., Thanou, M., Bell, J.D., Miller, A.D., 2009. Folate receptor targeted bimodal liposomes for tumor magnetic resonance imaging. Bioconjugate Chem. 20, 648–655.

Kasaai, M.R., Arul, J., Charlet, G., 2000. Intrinsic viscosity–molecular weight relationship for chitosan. J. Polym. Sci. Part B: Polym. Phys. 38, 2791–2798.

Kean, T., Roth, S., Thanou, M., 2005. Trimethylated chitosans as non-viral gene delivery vectors: cytotoxicity and transfection efficiency. J. Control. Release 103, 643–653.

Kim, S.H., Jeong, J.H., Cho, K.C., Kim, S.W., Park, T.G., 2005a. Target-specific gene silencing by siRNA plasmid DNA complexed with folate-modified poly(ethylenimine). J. Control. Release 104, 223–232.

Kim, S.H., Jeong, J.H., Joe, C.O., Park, T.G., 2005b. Folate receptor mediated intracellular protein delivery using PLL–PEG–FOL conjugate. J. Control. Release 103, 625–634.

Kim, Y.H., Gihm, S.H., Park, C.R., Lee, K.Y., Kim, T.W., Kwon, I.C., et al., 2001. Structural characteristics of size-controlled self-aggregates of deoxycholic acid-modified chitosan and their application as a DNA delivery carrier. Bioconjugate Chem. 12, 932–938.

Koping-Hoggard, M., Varum, K.M., Issa, M., Danielsen, S., Christensen, B.E., Stokke, B.T., et al., 2004. Improved chitosan-mediated gene delivery based on easily dissociated chitosan polyplexes of highly defined chitosan oligomers. Gene Ther. 11, 1441–1452.

Lee, D.W., Powers, K., Baney, R., 2004. Physicochemical properties and blood compatibility of acylated chitosan nanoparticles. Carbohydr. Polym. 58, 371–377.

Lee, E.S., Oh, K.T., Kim, D., Youn, Y.S., Bae, Y.H., 2007. Tumor pH-responsive flower-like micelles of poly(L-lactic acid)-b-poly(ethylene glycol)-b-poly(L-histidine). J. Control. Release 123, 19–26.

Lee, E.S., Gao, Z., Kim, D., Park, K., Kwon, I.C., Bae, Y.H., 2008. Super pH-sensitive multifunctional polymeric micelle for tumor pHe specific TAT exposure and multidrug resistance: in vivo efficacy. J. Control. Release 129, 228–236.

Lee, E.S., Na, K., Bae, Y.H., 2005. Super pH-sensitive multifunctional polymeric micelle. Nano Lett. 5, 325–329.

Lee, E.S., Shin, H.J., Na, K., Bae, Y.H., 2003. Poly(L-histidine)-PEG block copolymer micelles and pH-induced destabilization. J. Control. Release 90, 363–374.

Li, F., Liu, W.G., Yao, K.D., 2002. Preparation of oxidized glucose-crosslinked N-alkylated chitosan membrane and in vitro studies of pH-sensitive drug delivery behaviour. Biomaterials 23, 343–347.

Liang, B., He, M.L., Xiao, Z.P., 2008. Synthesis and characterization of folate-PEG-grafted-hyperbranched-PEI for tumor-targeted gene delivery. Biochem. Biophys. Res. 367, 874–880.

Lo, S.L., Wang, S., 2008. An endosomolytic Tat peptide produced by incorporation of histidine and cysteine residues as a nonviral vector for DNA transfection. Biomaterials 29, 2408–2414.

Low, P.S., Lee, R.J., 1995. Folate-mediated tumor cell targeting of liposome entrapped doxorubicin in vitro. Biochem. Biophys. Acta 1233, 134–144.

Lu, B., Wang, C.-F., Wu, D.-Q, Li, C., Zhang, X.-Z, Zhuo, R.-X., 2009. Chitosan based oligoamine polymers: synthesis, characterization, and gene delivery. J. Control. Release 137, 54–62.

Mansouri, S., Cuie, Y., Winnik, F., Shi, Q., Lavigne, P., Benderdour, M., Beaumont, E., Fernandesa, J.C., 2006. Characterization of folate chitosan-DNA nanoparticles for gene therapy. Biomaterials 27, 2060–2065.

Mao, S., Shuai, X., Unger, F., Simon, M., Bi, D., Kissel, T., 2004. The depolymerization of chitosan: effects on physicochemical and biological properties. Int. J. Pharm. 281, 45–54.

Megeeda, Z., Haidera, M., Lib, D., O'Malley, B.W., Cappellod, J., Ghandeharia, H., 2004. In vitro and in vivo evaluation of recombinant silk-elastinlike hydrogels for cancer gene therapy. J. Control. Release 94, 433–445.

Midoux, P., Monsigny, M., 1999. Efficient gene transfer by histidylated polylysine/multidrug resistance: in vivo efficacy. J. Control. Release 129, 228–236.

Morris, V.B., Neethu, S., Abraham, T.E., Pillai, C.K.S., Sharma, C.P., 2009. Studies on the condensation of depolymerized chitosans with DNA for preparing chitosan-DNA nanoparticles for gene delivery applications. J. Biomed. Mater. Res. B: Appl. Biomater. 89B, 282–292.

Mumper, R.J., Wang, J.J., Claspell, J.M., Rolland, A.P., 1995. Novel polymeric condensing carriers for gene delivery. Proc. Int. Symp. Control. Release Bioactive Mater. 122, 178–179.

Park, I.K., Jiang, H.L., Cook, S.E., Cho, M.H., Kim, S.I., Jeong, H.J., et al., 2004. Galactosylated chitosan (GC)-raft-poly(vinyl pyrrolidone) (PVP) as hepatocyte-targeting DNA carrier: in vitro transfection. Arch. Pharm. Res. Dec. 27, 284–289.

Patchornik, A., Berger, A., Katchalski, E., 1957. Poly-L-histidine. J. Am. Chem. Soc. 79, 5227–5230.

Petersen, H., Kunath, K., Martin, A.L., Stolnik, S., Roberts, C.J., Davies, M.C., Kissel, T., 2002. Star-shaped poly(ethylene glycol)-block-polyethylenimine copolymers enhance DNA condensation of low molecular weight polyethylenimines. Biomacromolecules 3, 926–936.

Ross, J.F., Chaudhuri, P.K., Ratnam, M., 1994. Differential regulation of folate receptor isoforms in normal and malignant tissues in vivo and in established cell lines. Physiologic and clinical implications. Cancer 73, 2432–2443.

Rekha, M.R., Sharma, C.P., 2009. Blood compatibility and in vitro transfection studies on cationically modified pullulan for liver cell targeted gene delivery. Biomaterials 30, 6655–6664.

Sato, T., Ishii, T., Okahata, Y., 2001. In vitro gene delivery mediated by chitosan: effect of pH, serum, and molecular mass of chitosan on the transfection efficiency. Biomaterials 22, 2075–2080.

Thakor, D.K., Teng, Y.D., Tabata, Y., 2009. Neuronal gene delivery by negatively charged pullulan–spermine/DNA anioplexes. Biomaterials 30, 1815–1826.

Thanou, M., Florea, B.I., Geldof, M., Junginger, H.E., Borchard, G., 2002. Quaternized chitosan oligomers as novel gene delivery vectors in epithelial cell lines. Biomaterials 23, 153–159.

Wang, C.Y., Huang, L., 1984. Polyhistidine mediates an acid-dependent fusion of negatively charged liposomes. Biochemistry 23, 4409–4416.

Yang, L., Li, J., Zhou, W., Yuan, X., Li, S., 2004. Targeted delivery of antisense oligodeoxynucleotides to folate receptor-overexpressing tumor cells. J. Control. Release 95, 321–331.

Zheng, Y., Cai, Z., Song, X., Chen, Q., Bi, Y., Li, Y., Hou, S., 2009. Preparation and characterization of folate conjugated *N*-trimethyl chitosan nanoparticles as protein carrier targeting folate receptor: *in vitro* studies. J. Drug Target. 17, 294–303.